PN
PHYTONUTRIENTS

Information available at: infor@phytonutrients.pk
PHYTONutrients
Journal home page: https://phytonutrients.pk/index.php/pn

Lyceum Publisher

Computational Characterization of Alkaloid RW47 Venoterpine: DFT, Drug-Likeness, and Target Prediction Insights for Therapeutic Potential

Muhammad Mujtaba[1]*, Qandeel Fatima[1], Manahil Fatima[1], Laiba Rashid[1]

Received: May 18, 2025
Accepted: June 14, 2025
Published: August 3, 2025
Volume: 04 I 2025
Article ID: pn.v4i1.49
https://doi.org/10.62368/pn.v4i1.49

[1] School of Chemistry, University of the Punjab, New Campus, Lahore, Punjab, Pakistan, 54590; mujtabakhan1813@gmail.com; fatimaqandeel2002@gmail.com; manahilf198@gmail.com; laibarashid591@gmail.com
*Correspondence: mujtabakhan1813@gmail.com

ABSTRACT: Venoterpine **(ARV)** is a naturally occurring alkaloid that has not been extensively studied by scientists, despite its structural novelty. Because of the increasing interest in natural products, there is a need to investigate **ARV's** drug-likeness, stability, and target specificity using modern computational techniques. SwissADME was used to evaluate drug-likeness, solubility, lipophilicity, and pharmacokinetic features, including gastrointestinal absorption, BBB permeability, P-glycoprotein interaction, and cytochrome P450 enzymes. B3LYP functional and 6-311G** basis set calculation was carried out to estimate the electronic properties (ionization potential, electron affinity, dipole moment, and electrophilicity index) and thermodynamic properties of **ARV**. SwissADME prediction indicated that **ARV** has desirable physicochemical properties, including favorable water solubility, balanced lipophilicity, high gastrointestinal absorption, and the ability to penetrate the blood-brain barrier. It also passed through several drug-likeness filters, such as the rule of five by Lipinski, signifying a good medicinal chemistry prospect. DFT calculations showed an ionization potential of -6.6537 eV, an electron affinity of -0.6989 eV, and a HOMO-LUMO energy gap of 5.9548 eV, which suggested that it is electronically stable under biological conditions. SwissTargetPrediction demonstrated, it is capable of potential interaction with a wide range of protein classes, including oxidoreductases (33%), cytochrome P450 enzymes (13%), kinases (13%), lyases (20%), membrane receptors (6.7%), and unspecified proteins (6.7%), which promises versatile pharmacological applications. The integrated in silico assessment of **ARV** reveals a strong drug-like profile with electronic stability, good pharmacokinetics, and the ability to interact with a wide range of biological targets. These results suggest that **ARV** is a promising candidate for further experimental research in drug development.

Keywords: Venoterpine; SwissADME analysis; Physiochemical properties; DFT calculations; Molecular docking

1. Introduction

Nature has traditionally functioned as a resource for drug development, providing an extensive collection of bioactive molecules with a variety of chemical structures and pharmacological properties (Atanasov et al., 2021). Medicinal plants have long been used in traditional medicine systems around the world, and more

than 80% of approved medications are derived from or inspired by natural substances, demonstrating their continued significance in pharmacotherapy (Sneader, 1996). Alkaloids are naturally occurring organic molecules, contain a nitrogen atom in their aromatic ring (Ansari et al., 2023). These molecules are derived from plants and display various biological effects, including analgesic, antiarrhythmic, and anticancer actions (Bhadra and Kumar, 2011). They are useful leads in drug development because of their intricate frameworks and interactions with biological targets. Throughout history, alkaloids have been essential to medicine; morphine and quinine, for example, are the building blocks of contemporary medications (Kittakoop et al., 2014). Alkaloids have attracted increased interest as therapeutic agents due to recent developments in pharmacognosy, which address new health issues like cancer, neurological diseases, and antibiotic resistance (Olofinsan et al., 2023).

Computer-aided drug discovery (CADD) uses computer approaches to speed up and refine the selection of prospective therapeutic options. These techniques enable researchers to simulate protein-ligand interactions, predict binding affinities, and optimize pharmacological profiles (Macalino et al., 2015). In modern drug discovery, computational approaches are essential for assessing the pharmacokinetic and physicochemical features of potential therapeutic medicines. Among these, in silico ADME profiling is used as a prediction technique to analyze a compound's drug-likeness and pharmacokinetic behavior, which helps to streamline the preclinical evaluation process (Bakchi et al., 2022). In addition to ADME profiling, Density Functional Theory (DFT) has emerged as an important quantum mechanical technique in drug design. DFT makes it easier to investigate a molecule's electronic structure, allowing users to anticipate attributes like electronic density, molecular orbitals, and energy levels. These findings are critical for understanding a compound's reactivity, stability, and potential interactions with biological targets (De Proft and Geerlings, 2001). Researchers can acquire a comprehensive view of a compound's pharmacological profile by combining DFT analysis with ADME profiling, which improves the rational design and optimization of novel treatments (Atrushi et al., 2023).

Venoterpine, or alkaloid RW47 (AVR), is a pyridine alkaloid having the chemical formula $C_9H_{11}NO$ (Cordell, 1977). It has been found in a variety of plant species, most notably in Camptotheca acuminata, a deciduous tree endemic to China that belongs to the Cornaceae family. C. acuminata has been used in traditional Chinese medicine for a variety of medicinal purposes, owing to its high concentration of bioactive chemicals, which include the well-known anticancer agent camptothecin (Paladhi et al., 2023). Venoterpine, being a member of an alkaloid class, has received interest for its potential biological properties (Alaei Faradonbeh, 2017). Literature indicates that Venoterpine has physicochemical features suitable for drug development. Despite its promising pharmacological profile and structural similarity to various bioactive alkaloids, Venoterpine (ARV) remains largely uninvestigated for its therapeutic potential using computational approaches. These qualities necessitate additional research into its pharmacological potential and prospective applications in drug discovery.

In this study, we investigate Venoterpine (RW47)'s physicochemical features, electrical characteristics, and possible biological targets using DFT calculations and in silico ADMET profiling to provide a full grasp of this compound's therapeutic potential. While the results provide useful computational insights into RAV's potential, however, the research is limited to computational methods and therefore cannot reproduce the complexity of biological systems. Experimental validation is needed to adequately predict other properties such as metabolic stability, bioavailability, toxicity, and off-target effects. Besides, the SwissTargetPrediction tool provides estimations as probabilities and hence may miss novel or astonishing targets.

2. Methodology

2.1. ADME Analysis

For ADME analysis, the SwissADME web tool (http://www.swissadme.ch/) was used. Ligand SMILE was retrieved from the KNApSAck database (https://www.knapsackfamily.com/knapsack_core/top.php). It was then uploaded to SwissADME software for evaluation of ADME (absorption, distribution, metabolism, and excretion) analysis.

2.2. Density Functional Theory (DFT) Calculations

The Gaussian 09W software package was used for Density Functional Theory (DFT) calculations. The geometry optimization and energy minimization of the phytonutrient were carried out at the B3LYP level using a 6-311G**

basis set using Gaussian 09W software (https://gaussian.com/glossary/g09). The default settings were used for the Gaussian calculation in the gaseous phase. Drawing molecular structure, setting up input file, and analysis of optimized geometry were done using GaussView 6.0. Using HOMO-LUMO energies, the chemical reactivity descriptors were calculated using the following equations. Global reactivity descriptors such as ionization potential, electron affinity, chemical hardness, softness, electronegativity, were calculated based on the frontier molecular orbital energies (HOMO and LUMO) derived from DFT calculations. These parameters were calculated using well-known theoretical relationships grounded in Koopmans' theorem and conceptual density functional theory (DFT), as described in the literature (Koopmans, 1934).

2.3. Biological Target Prediction

The probable biological targets of the ligand were determined using the SwissTargetPrediction web tool (http://www.swisstargetprediction.ch/). SMILES format of the ligand was submitted to the software, and checked for targets in Homo sapiens. The output file contained the list of predicted targets along with their probability score. The results are also shown in the form of a pie chart.

Table 1: Name, SMILE, KNApSAck_ID, and Structures of the Studied Compound

Compound	SMILE	C_ID	Structure
Alkaloid RW47 Venoterpine **(ARV)**	C[C@@H]1c2cnccc2C[C@@H]1O	C00054142	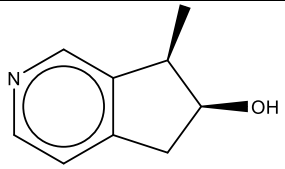

3. Results

3.1. ADME Analysis

3.1.1. Physicochemical properties

The **ARV** molecule's potential as a bioactive molecule is demonstrated by its physicochemical profile in **Table 2**. **ARV**, a relatively tiny molecule with a molecular weight of 149.19 g/mol and a molecular formula of $C_9H_{11}NO$, favors oral bioavailability and membrane permeability. It contains 11 heavy atoms and 6 aromatic atoms in its structure. By striking a balance between rigidity and flexibility, the fraction of sp^3-hybridized carbon atoms (0.44) indicates moderate molecular complexity. Since **ARV** lacks rotatable bonds, it appears to have a stiff structure that could improve binding selectivity. Due to its two hydrogen bond acceptors and one hydrogen bond donor, it may interact well with biological receptors and falls within the ideal range for drug-likeness. The topological polar surface area (TPSA) of 33.12 Å² and the molar refractivity of 42.83 further indicate appropriate size and polarizability for pharmacokinetic compatibility.

Table 2. Physicochemical Properties of **ARV**

Property	Value
Formula	$C_9H_{11}NO$
Molecular weight	149.19 g/mol
Number of heavy atoms	11
Number of aromatic heavy atoms	6
Fraction Csp^3	0.44
Number of rotatable bonds	0
Number of H-bond acceptors	2
Number of H-bond donors	1
Molar Refractivity	42.83
TPSA (Topological Polar Surface Area)	33.12 Å²

3.1.2. Lipophilicity

With a consensus Log Po/w of 1.22, the compound's lipophilicity falls within the ideal range for oral medications. Predictions from each model varied from 0.86 (XLOGP3) to 1.71 (SILICOS-IT), as shown in **Table 3**. A balanced hydrophilic-lipophilic nature is indicated by these moderate LogP values, which promote adequate membrane permeability without excessive fat solubility that could impair

bioavailability or cause accumulation in adipose tissues.

3.1.3. Solubility

According to solubility predictions, the molecule is very soluble in a variety of models. The Ali model provides a greater solubility estimate (10.8 mg/mL), but the ESOL model predicts a Log S of 1.71, or 2.91 mg/mL. 0.972 mg/mL, or a Log S of –2.19, is the result of the SILICOS-IT model. The molecule has adequate aqueous solubility for formulation in aqueous medium and efficient absorption, according to the values shown in **Table 4**.

3.1.4. Pharmacokinetics

Table 5 shows the molecule's pharmacokinetic profile, pointing to advantageous distribution and absorption characteristics. The chemical may be suitable for oral delivery because of its high gastrointestinal (GI) absorption. It can also cross the blood-brain barrier (BBB), which is important for activation of the central nervous system.

Table 3. Lipophilicity of **ARV**

Log Po/w Method	**Value**
iLOGP	1.56
XLOGP3	0.86
WLOGP	1.10
MLOGP	0.87
SILICOS-IT	1.71
Consensus Log Po/w	1.22

Table 4. Solubility of **ARV**

Method	**Log S**	**Solubility (mg/mL / mol/L)**	**Class**
ESOL	-1.71	2.91e-01 mg/mL; 1.95e-02 mol/L	Very soluble
Ali	-1.14	1.08e+01 mg/mL; 7.26e-02 mol/L	Very soluble
SILICOS-IT	-2.19	9.72e-01 mg/mL; 6.52e-03 mol/L	Soluble

The chemical reduces the possibility of metabolic drug–drug interactions by not being a substrate of P-glycoprotein (P-gp) and by not inhibiting the main cytochrome P450 (CYP) isoforms, such as CYP1A2, CYP2ARV9, CYP2C9, CYP2D6, and CYP3A4. Transdermal absorption potential is comparatively low, as indicated by the log Kp (skin permeation) value of -6.60 cm/s.

3.1.5. Drug- Likeliness

After being evaluated against the main drug-likeness standards, the molecule was found to have good oral bioavailability and to comply with Lipinski's criterion without any violations. However, because of its relatively low molecular weight, one violation was noted for each of the Ghose (MW <160) and Muegge (MW <200) filters. The chemical supports favorable oral bioavailability by meeting the Veber and Egan criteria. A bioavailability score of 0.55 indicates a moderate potential for oral bioavailability **Table 6.**

Table 5. Pharmacokinetic Properties of **ARV**

Property	**Value**
GI absorption	High
BBB permeant	Yes
P-gp substrate	No
CYP1A2 inhibitor	No
CYP2ARV9 inhibitor	No
CYP2C9 inhibitor	No
CYP2D6 inhibitor	No
CYP3A4 inhibitor	No
Log Kp (skin permeation)	-6.60 cm/s

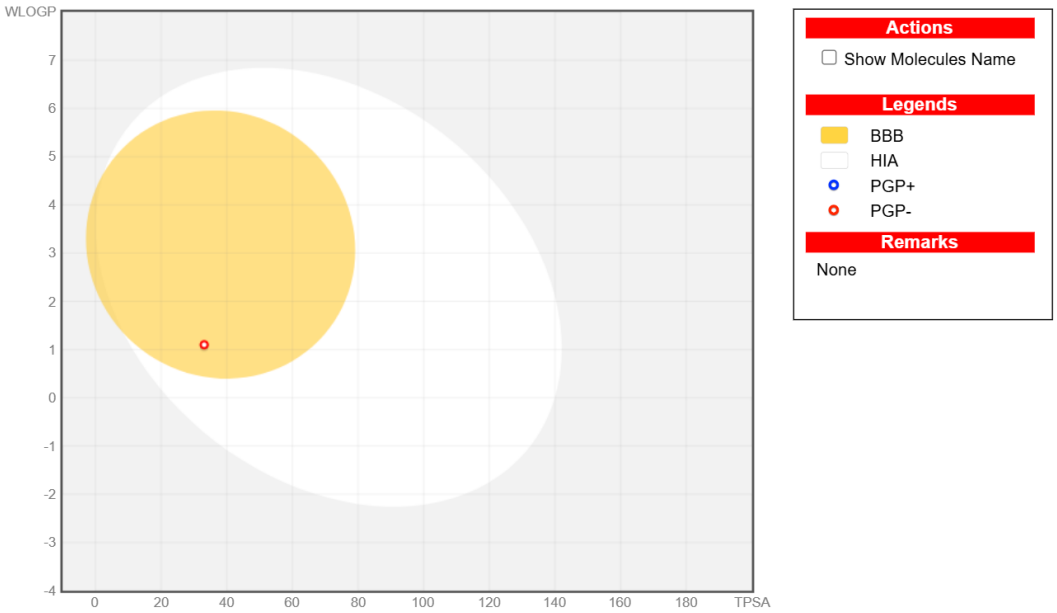

Figure 1: BOILED-Egg model of molecule **ARV** illustrating its pharmacokinetic profile. The molecule is positioned within the yolk, indicating blood–brain barrier (BBB) permeability, and within the white region, indicating high Gastrointestinal (GI) absorption. Its location outside the P-gp substrate region suggests it is not a substrate for P-glycoprotein-mediated efflux.

Table 6. Drug-Likeness Evaluation of **ARV**

Rule	**Result**
Lipinski	Yes; 0 violation
Ghose	No; 1 violation: MW<160
Veber	Yes
Egan	Yes
Muegge	No; 1 violation: MW<200
Bioavailability Score	0.55

3.1.6. Medicinal Chemistry

The molecule exhibited zero PAINS and Brenk alerts, indicating an absence of structural features commonly associated with false-positive biological activity and toxicity risks, respectively. As the compound's molecular weight was less than 250 Da, it failed to satisfy the lead-likeness requirements; nevertheless, this is a relatively small infraction that does not necessarily rule out **ARV** as a drug-like contender. Additionally, **ARV's** synthetic accessibility score of 2.57 indicates that it is easily synthesized, which increases its attractiveness for additional experimental and medicinal chemistry research **Table 7**.

Table 7: Medicinal Chemistry of **ARV**

Property	**Value**
PAINS	0 alert
Brenk	0 alert
Leadlikeness	No; 1 violation: MW<250
Synthetic accessibility	2.57

3.2 Density functional theory calculations

3.2.1. Chemical Reactivity Descriptors

To evaluate the **AVR's** chemical behavior, specifically its stability, reactivity, and potential for electron transfer interactions, its electronic and reactivity parameters were calculated. With an electron affinity (A) of -0.6989 eV and an ionization potential (I) of -6.6537 eV, the HOMO–

LUMO energy gap (ΔE) was 5.9548 eV, suggesting a less reactive and more stable molecule.

The tendency of the electron cloud to escape from the molecule was reflected in the chemical potential (μ), which was found to be –3.6763 eV. According to calculations, the chemical hardness (η) and softness (S) were 2.9774 eV and 0.3358 eV^{-1}, respectively. These values indicate a balanced reactivity profile and modest resistance to charge transfer.

A moderately electrophilic nature was indicated by the electrophilicity index (ω), which was found to be 2.2696. Additionally, the molecule displayed values of 4.4799 for nucleophilic assault (ω^-) and 0.8036 for electrophilic attack (ω^+), indicating a greater propensity to receive electrons as opposed to donating them. Additionally, the maximum charge transfer (ΔNmax) was 0.6173, showing a considerable ability to exchange electron density with its surroundings, and the electronegativity (χ) was calculated to be 3.6763 eV, which is consistent with the chemical potential. Electron back-donation processes contributed favorably to the back-donation energy, which was -0.7443 eV **Table 8.**

Table 8. Global Reactivity Descriptors of **ARV**

Parameter	**Value**
Ionization Potential (I) **(eV) (-H)**	-6.6537
Electron Affinity (A) **(eV) (-L)**	-0.6989
Energy Gap (ΔE) **(eV)**	5.9548
Chemical Potential (μ) **(eV)**	-3.6763
Hardness (η) **(eV)**	2.9774
Softness (S) **(eV^{-1})**	0.3358
Electrophilicity Index (ω) **(eV)**	2.2696
Electrophilicity Index (ω+) **(au)**	0.8036
Electrophilicity Index (ω-) **(au)**	4.4799
Electronegativity (χ) **(eV)**	3.6763
Back-donation Energy **(eV)**	-0.7443
Maximum Electron Transfer **(eV)** (ΔNmax)	0.6173

H (–I): highest occupied molecular orbital energy (HOMO), **L (–A)**: lowest unoccupied molecular orbital energy (LUMO), **ΔE** (L–H): energy gap (HOMO-LUMO gap), **μ**: chemical potential, **η**: chemical hardness, **S**: chemical softness, **ω:** electrophilicity index, ω^+: electron donating power, ω^-: electron accepting power, **ΔNmax**: maximum number of electrons transferred, $\Delta\varepsilon_{back\text{-}donat}$: back-donation energy.

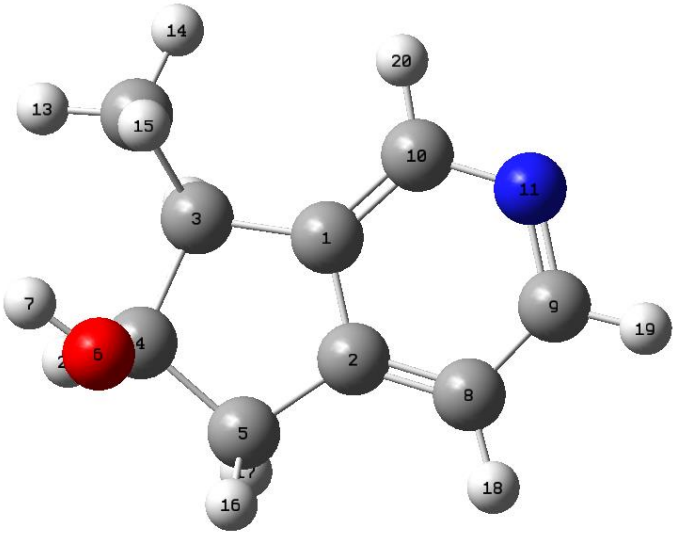

Figure 2: Optimized geometry of ARV

3.2.2. Thermodynamic Properties

The **ARV's** polarizability, thermochemical quantities, and dipole moment are shown in **Table 9.** The main thermodynamic quantities for the **ARV** are ΔE, ΔH, and ΔG, which are -479.3407, -479.3305, and -479.3749 au, respectively. The Δ $E_{thermal}$ value of the molecule is also 121.964 (kcal/mol). The **ARV** has the lowest entropy value, with the 93.405 cal/mol K coming in second. The Cv (cal/mol K) quantity of the compounds is 36.778, according to the table. The DM (in Debye) value of the compound is determined to be 3.6290. Nonetheless, the calculated α (au) values of the compounds are 99.5296.

Table 9. Thermodynamic Properties of **ARV**

Parameters	**Values**
ΔE(au)	-479.3407
ΔH(au)	-479.3305
ΔG (au)	-479.3749
$\Delta E_{thermal}$ (kcal/mol)	121.964
Cv (cal/molK)	36.778
S (cal/molK)	93.405
DM (debye)	3.6290
α (au)	99.5296

ΔE: electronic energy, **ΔH**: enthalpy, **ΔG**: gibbs free energy, **$\Delta E_{thermal}$**: thermal energy, **Cv**: heat capacity at constant volume, **S:** entropy, **DM**: dipole moment, **α**: polarizability.

3.2. Frontier molecular orbital and Molecular Electrostatic Potential (MEP)

When predicting a compound's chemical and antioxidant activity, frontier molecular orbitals (FMOs), which are represented by the lowest unoccupied molecular orbital (LUMO) and the highest occupied molecular orbital (HOMO), are crucial. The Molecular Electrostatic map in **Figure 4** is presented along with the HOMO and LUMO **Figure 3**.

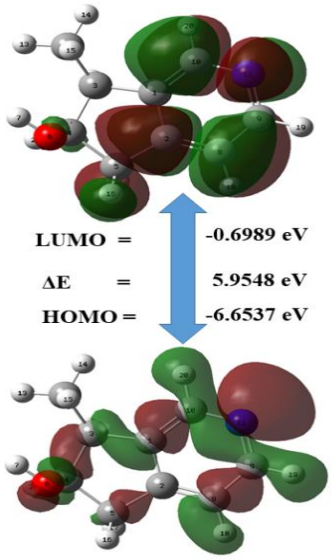

Figure 3: Frontier molecular orbitals of molecule **ARV.** The highest occupied molecular orbital (HOMO) and the lowest unoccupied molecular orbital (LUMO) distributions illustrate the electron-rich and electron-deficient regions, providing insight into the molecule's reactivity, charge transfer potential, and chemical stability.

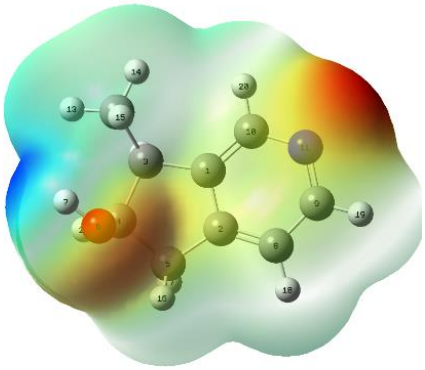

Figure 4: Molecular electrostatic potential (MEP) map of molecule **ARV.** The surface illustrates the spatial distribution of electrostatic charge, highlighting electron-rich and electron-deficient regions, which are critical for predicting sites of electrophilic and nucleophilic interactions.

3.3. Biological Targets Prediction

For **ARV**, the Target Prediction analysis showed that 33.3% of the projected targets are enzymes, with oxidoreductases (20%), cytochrome P450 enzymes (13.3%), and lyases (13.3%) coming in second and third, respectively. Membrane receptors, kinases, and unidentified proteins all showed slight interactions (each 6.7%). This distribution highlights **ARV's** possible role in metabolic and oxidative processes by indicating that it mostly interacts with enzymatic and redox-related proteins **Figure 5**.

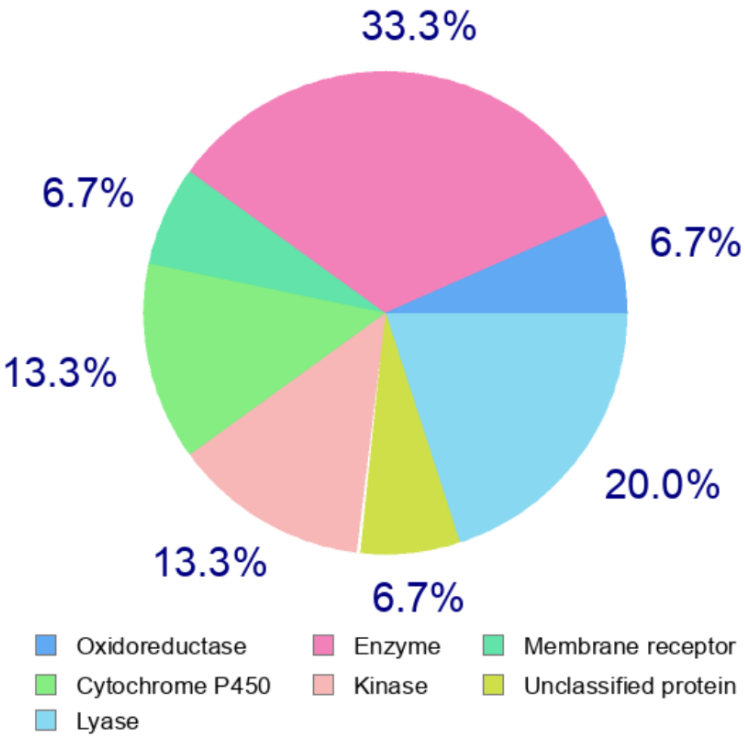

Figure 5: Predicted Biological Target of **ARV**

4. Discussions

SwissADME utilized the Lipinski Rules of five to select drug-likeness descriptors. The Lipinski's rule of five suggests that a molecule with a molecular weight (MW) < 500 Da, less than 10 hydrogen bond acceptors (nHBA), and less than 5 hydrogen bond donors (nHBD), shows good permeation or absorption (Vlad et al., 2020). Similarly, molecular weight is one of the factors that determines the drug permeability of a compound. Central nervous disease needs drugs with a small molecular weight to reach its target than other diseases. Therefore, for better permeability and good intestinal absorption, a molecular weight of < 450 is suggested (Atkinson et al., 2002). The compound adheres to Lipinski's rule of five, having a molecular weight less than 500 Da, and fewer nHBD and nHBA than the required threshold. Fsp3, which is the ratio of sp3 carbon to total carbon atoms, shows how saturated a molecule is with carbon atoms and how complicated the spatial structure is (Lovering et al., 2009). As 84% of commercially available medications satisfy this criterion, ADMELab states that a Fsp3 value greater than 0.42 is deemed appropriate. Strong drug likelihood is indicated by **ARV**, which has the Fsp3 value of 0.44. A high Fsp3 score is not a characteristic of high-quality medicines and complicates chemical production (Kombo et al., 2013).

Furthermore, compounds having rotatable bonds more than 10 tend to be more flexible and have higher entropy, which makes it harder for the body to absorb them, flexible, useful, and simple**.** While a TPSA of 60 $Å^2$ would result in strong absorption with fractional absorption over 90%, a certain molecular system with a TPSA of 140 $Å^2$ would have low absorption with fractional absorption less than 10% (Daina et al., 2017). The potential bioavailability of **ARV** is supported by its Topological Polar Surface Area (TPSA) of 33.12 $Å^2$. SwissADME uses iLOGP, XLOGP3, WLOGP, MLOGP, and SILICOS-IT to assess lipophilicity (Cheng et al., 2007). The arithmetic mean of the numbers derived from these five approaches is the consensus Log P o/w. Solvation free energies in water and n-octanol are determined using the physical method known as iLOGP, which uses the generalized Born and solvent accessible surface area (GB/SA) methodology. The compound **ARV** has a consensus Log P o/w of 1.22, which indicates the best lipophilic properties (optimal range: 0 – 5). A medication molecule's absorption in the human body is predicted by its water solubility, lipophilicity, and human intestinal absorption (HI). The compound's solubility is greatly influenced by the solvent's composition, ambient temperature, and pressure. Insoluble < -10, poorly soluble < -6, moderately soluble < -4, very soluble < -2, and soluble < 0 are the solubility predictions made by SwissADME (Savjani et al., 2012). The compound **ARV** has a water solubility of -1.71, falling between -1 and 0.5 mol/L, which is the ideal range. The compound demonstrated good gastrointestinal (GI) absorption. The Boiled Egg model, which evaluates the GI passive absorption and brain access by passive diffusion, depicts an elliptical region populated by well-absorbed molecules. The yellow yolk region predicts the molecules that are likely to penetrate the brain, whereas the white region consists of the molecules that are more likely to show good GI tract absorption. If a medicine is absorbed via a method other than the oral route, it would be seen in the gray region of the chart (Daina and Zoete, 2016).

Distribution of a drug molecule can be examined by considering Blood Brain Barrier (BBB) permeability, glycoprotein P (P-gp), and the fraction of unbound descriptors. The blood-brain barrier is a complicated structure that separates the Central Nervous System (CNS) from its peripheral tissues. It controls the transfer of cells, materials, and nutrients from blood to the brain and vice versa (Małkiewicz et al., 2019). P-gp is a complex ATP-dependent drug extraction pump that is found in numerous human tissues. **ARV** molecule shows BBB penetration, which means it is not free of CNS toxicity. It also helps in the removal of toxins and cellular metabolites from the brain. The **ARV** molecule is not a substrate of p-glycoproteins. This may not connect it to interactions with different external or endogenous substances, including drugs. The pharmacological profile of other drugs might not be affected because it is expected that the **ARV** will not interact with P-glycoprotein (Zhang et al., 2021). The blood level for another medication that is a substrate for the target enzyme can be raised or lowered by metabolic enzyme inducers or inhibitors. This may result in several pharmacokinetic medication interactions with inducers or inhibitors of CYP (Bolleddula et al., 2021). The compound's metabolism was predicted by estimating the inhibition of the P450 superfamily's primary cytochromes (CYP). The process entails CYP enzyme inhibition and is the

main mechanism for metabolism-based drug-drug interaction. These cytochromes include CYP1A2, CYP2C9, CYP2ARV9, CYP2D6, and CYP3A4. The biotransformation or excretion of all therapeutically used medications, including some anticancer agents, is exploited by enzyme inhibition, which raises the drug's plasma level and influences the clinical outcome. The retarded effect is shown in case of prodrug (Manikandan and Nagini, 2018). Inhibition of CYPs may result in toxicity or decreased medication effectiveness. One important enzyme that breaks down medications with a low therapeutic index is CYP2C9, while CYP2D6 is a highly complex and polymorphic structure involved in metabolization. Its deficiency can result in decreased drug efficiency or an increased risk of harmful effects (Domínguez-Villa et al., 2021). CYP2ARV9 helps with the metabolization of many pharmaceuticals and the detoxification of dangerous carcinogens. Most medications are metabolized by CYP3A4, the most important isomorph of CYP P450, which is unaffected by endogenous chemicals (Zhou, 2008). The **ARV** molecule is projected to behave similarly, with no effect on CYP enzymes. The ability of a molecule to function as the lead in drug production is known as lead-likeliness**.** Veber et al. proposed that for better absorption or permeation, a molecule must have a polar surface area (PSA) < 140 $Å^2$ and fewer than 10 rotatable bonds (NBR) < 10 (Małkiewicz et al., 2019). ARV does not show any violation of the Lipinski and Veber rules. Ghose filter's rules predict the likeness of a molecule to be a drug if it has a molecular weight (MW) in the range of 160-480 Da, molar refractivity between 40 and 130, total number of atom, including hydrogen bond donors and acceptors, ranging from 20 to 70, and predicted Log P value within the limit of -0.4-5.6 (Rashid et al., 2021). Similarly, according to Muegge filter's rules, for a molecule to possess desirable pharmacokinetic properties, it must have molecular weight (MW) between 200 and 600 Da, more than 4 carbon atoms, polar surface area (PSA) <150 $Å^2$, not more than 7 rings, predicted Log P value between -2 and 5, number of rotatable bonds (NBR) ≤ 15, at least one heteroatoms, less than 5 hydrogen bond donors (nHBD) and less than 10 hydrogen bond acceptors (nHBA) (Yadav et al., 2021). ARV has the molecular weight of 149.19 g/mol and exhibits one violation of both Ghose and Muegge rules. Nevertheless, it complies with all other criteria, which suggests that it would show excellent absorption or permeation.

Synthetic accessibility (SA) score reflects the ease of synthesizing a drug. **ARV** has an SA score of 2.57, suggesting its undemanding laboratory synthesis. It showed 0 PAIN alerts, indicating no association with reactive compounds, α-screen artefacts, and frequent hitters (Sharma et al., 2025). However, PAIN alerts are insufficient to classify a molecule suitable for therapeutic applications; further research is needed. No Brenk alerts are associated with **ARV**, which makes it a safe and non-reactive therapeutic candidate.

The HOMO LUMO values of the compound were calculated as -6.6537 and -0.6989 eV, while, the HOMO–LUMO energy gap of 5.9548 eV was calculated. This larger energy gap indicates that the molecule has low intrinsic reactivity, good thermodynamic stability inside a biological system. In theory, E_{HOMO} is a useful measure of the ability to scavenge free radicals (Zheng et al., 2017). Similarly, a high ΔE value is proportional to high hardness values. Likewise, a ligand with a low ΔE value will have a high softness, and the ligand is considered is soft ligand (Eşme and Sağdınç, 2018)**.** Chemical hardness is a measure of an atom's resistance to a charge transfer. The distance between HOMO and LUMO molecular orbitals is connected with chemical hardness, which is based on border molecular orbital (Mebi, 2011). The softness of the molecule is implied by a tiny energy gap between the LUMO and HOMO, whereas the hardness is shown by a big gap. Compared to a hard molecule, a soft molecule is more reactive and can give electrons to the recipient more readily (Shahab and Sheikhi, 2020). With a significant degree of electron polarizability, or softness (S = 0.3358), the molecule has a chemical hardness of 2.9774, which improves its ability to donate electrons and its overall reactivity. Its computed chemical potential (μ = –3.6763 eV) and electronegativity (χ = 3.6763 eV) demonstrate thermodynamic stability and a balanced electron-attracting propensity. Similarly, the electrophilicity index (ω) is a crucial chemical descriptor, which presents the ability of a ligand to accept electrons (ω = 2.2696) (Singh et al., 2021). There is a clear preference for nucleophilic (electron-donating) interactions, as seen by the nucleophilic attack index (ω^- = 4.4799), which is much higher than the electrophilic attack index (ω^+ = 0.8036). Furthermore, the molecule's back-donation energy (–0.7443 eV) and maximum charge transfer capacity (ΔN_{max} = 0.6173) highlight its aptitude for taking part in electron transfer operations. All of these electrical characteristics

point to **ARV** as a highly reactive and adaptable molecule that may be able to participate in antioxidant processes and scavenge free radicals, which could promote its use in protective or therapeutic applications. The free energy and enthalpy values can be used to determine the spontaneous nature of a reaction and the stability of a product.

Negative values are better for thermal stability and favor antioxidant ability (Cohen and Benson, 1993). Negative values of ΔH and ΔG, -479.3305 au and -479.3749 au, respectively, for ARV signify that the molecule is thermally stable and formation might be spontaneous under standard conditions. The dipole moment affects non-bonded interactions and the smooth development of hydrogen bonds in computational molecular modeling. Increasing the dipole moment can also improve the binding property (Lien et al., 1982). Dipole moment of 3.6290 Debye suggests a considerable separation of charges, leading to a polar nature of the molecule, which makes it soluble in polar solvents through dipole-dipole interactions or hydrogen bonding. Higher polarizability is related to better intermolecular interactions and better chemical reactivity. It indicates the responsiveness of the molecule's electronic cloud to external electric fields (Tandon et al., 2021). The moderate-to-strong ability of **ARV** to stabilize transitory states during intermolecular interactions is suggested by its polarizability, which is beneficial for interacting with protein targets. The figure shows that the HOMO is (**Figure 3**) mostly spread over the electron-dense region, especially near the nitrogen atom and adjacent conjugated system, indicating a nucleophilic site. LUMO, on the other hand, is localized over the electron-deficient, particularly, the carbonyl center, showing an electrophilic character. These HOMO, LUMO and MEP diagrams play an important role in determining the possible reactive site of a molecule (Serin, 2022). The shape of the HOMO dictates the locations for free radical assault, therefore molecules with lower E_{HOMO} are more stable and less likely to donate electrons.

The molecular electrostatic potential map (**Figure 4**) confirms the polarity of the molecule and its possible hydrogen bonding contact sites by highlighting electron-rich and electron-deficient zones close to the oxygen and hydrogen atoms, respectively. These maps support the **ARV's** moderate electrophilic and nucleophilic behavior and appropriateness as a lead compound. The MEP is typically represented having red, yellow, blue, and green regions. The red area shows electron-rich, the blue shows slightly electron-deficient, the yellow shows slightly electron-rich region, the green shows neutral region, and the blue region shows positive region. The potential increase in order of red, orange, yellow, green, and blue. It is related to the electronic density and beneficial for the identification of electrophilic and nucleophilic sites along with hydrogen-bonding interactions (Eşme and Sağdınç, 2018). The SwissTargetPrediction tool shows a wide range of possible biological interactions. The projected distribution of the target protein class is depicted in the pie chart. Since a sizable fraction of targets (33.3%) belong to the general enzyme category, it shows that **ARV** may influence important metabolic or regulatory processes through a variety of enzymatic interactions. 20% of the anticipated targets are oxidoreductases. Redox equilibrium, the control of oxidative stress, and the regulation of metabolic energy all depend on these enzymes. Given its electrophilicity and softness indices, which indicate its capacity to donate electrons, **ARV** may be a good candidate for interactions with oxidoreductases, suggesting possible antioxidant activity (Finkel, 2011).

Notable anticipated targets also include cytochrome P450 enzymes (13.3%). This increases the importance of **ARV** in pharmacological or nutraceutical uses by indicating that it might be engaged in metabolic processing pathways (Guengerich, 2008). Furthermore, membrane receptors (6.7%) and lyases (13.3%) are noted as secondary targets. The presence of lyases suggests that **ARV** may be able to catalyze bond cleavage processes without oxidation or hydrolysis. Finally, the existence of proteins whose function or categorization is still being studied, or a small regulatory interaction potential, is shown by 6.7% of kinases and 6.7% of unclassified proteins. Considering all these properties, **ARV's** anticipated interaction profile points to a multi-targeted nature. More in vitro and in vivo validation investigations are necessary in light of these findings, which suggest its potential utility in metabolic modulation, antioxidant mechanisms, and potentially even medicinal development.

5. Conclusion

In summary, the current in silico investigation provides a detailed picture of the **AVR**. The SwissADME analysis shows promising pharmacokinetic properties, indicating good bioavailability, excellent solubility, lipophilicity, and satisfactory physicochemical properties. It

also suggested that the compound can cross the blood-brain barrier and thus can be used in CNS/brain-related diseases. Furthermore, the DFT calculations show that the compound is stable due to a large HOMO-LUMO gap (5.9548 eV) and high chemical hardness (2.9774 eV). The high value of chemical potential and moderate electrophilicity suggest thermodynamic stability of the compound. Similarly, the high nucleophilicity index shows strong nucleophilic behavior. Computational target prediction suggests diverse activity of the compound, and may interact primarily with oxidoreductases, lyases, and other enzymes. These combined computational findings offer a strong foundation for future research. The computational studies have some limitations, and experimental investigation is required to validate the predicted ADME properties, explore the molecule's interactions with the identified targets, and ultimately assess its therapeutic potential.

Author Contributions: Muhammd Mujtaba: supervision, methodology; investigation and draft writing/editing. Qandeel Fatima: Methodology; investigation and initial draft writing. Manahil Fatima: Methodology; investigation and initial draft writing. Laiba Rashid: Methodology; investigation and initial draft writing.

Funding: This research received no external funding.

Acknowledgements: Nil.

Conflicts of Interest: The author declare no conflict of interest.

References

Alaei Faradonbeh, D., 2017. Natural drugs in the treatment and prevention of prostate diseases.

Ansari, M.F., Khan, H.Y., Tabassum, S., Arjmand, F., 2023. Advances in anticancer alkaloid-derived metallo-chemotherapeutic agents in the last decade: Mechanism of action and future prospects. Pharmacology & therapeutics 241, 108335.

Atanasov, A.G., Zotchev, S.B., Dirsch, V.M., Supuran, C.T., 2021. Natural products in drug discovery: advances and opportunities. Nature reviews Drug discovery 20(3), 200-216.

Atkinson, F., Cole, S., Green, C., Van de Waterbeemd, H., 2002. Lipophilicity and other parameters affecting brain penetration. Current Medicinal Chemistry-Central Nervous System Agents 2(3), 229-240.

Atrushi, K.S., Ameen, D.M., Abdulrahman, S.H., Abachi, F.T., 2023. Density functional theory, ADME, and molecular docking of some anthranilic acid derivatives as cyclooxygenase inhibitors. J. Med. Chem. Sci 6, 1943-1952.

Bakchi, B., Krishna, A.D., Sreecharan, E., Ganesh, V.B.J., Niharika, M., Maharshi, S., Puttagunta, S.B., Sigalapalli, D.K., Bhandare, R.R., Shaik, A.B., 2022. An overview on applications of SwissADME web tool in the design and development of anticancer, antitubercular and antimicrobial agents: a medicinal chemist's perspective. Journal of Molecular Structure 1259, 132712.

Bhadra, K., Kumar, G.S., 2011. Therapeutic potential of nucleic acid-binding isoquinoline alkaloids: Binding aspects and implications for drug design. Medicinal research reviews 31(6), 821-862.

Bolleddula, J., Ke, A., Yang, H., Prakash, C., 2021. PBPK modeling to predict drug-drug interactions of ivosidenib as a perpetrator in cancer patients and qualification of the Simcyp platform for CYP3A4 induction. CPT: pharmacometrics & systems pharmacology 10(6), 577-588.

Cheng, T., Zhao, Y., Li, X., Lin, F., Xu, Y., Zhang, X., Li, Y., Wang, R., Lai, L., 2007. Computation of octanol− water partition coefficients by guiding an additive model with knowledge. Journal of chemical information and modeling 47(6), 2140-2148.

Cohen, N., Benson, S.W., 1993. Estimation of heats of formation of organic compounds by additivity methods. Chemical Reviews 93(7), 2419-2438.

Cordell, G.A., 1977. Chapter 8 The Monoterpene Alkaloids, in: Manske, R.H.F. (Ed.) The Alkaloids: Chemistry and Physiology. Academic Press, pp. 431-510.

Daina, A., Michielin, O., Zoete, V., 2017. SwissADME: a free web tool to evaluate pharmacokinetics, drug-likeness and medicinal chemistry friendliness of small molecules. Scientific reports 7(1), 42717.

Daina, A., Zoete, V., 2016. A boiled-egg to predict gastrointestinal absorption and brain penetration of small molecules. ChemMedChem 11(11), 1117-1121.

De Proft, F., Geerlings, P., 2001. Conceptual and computational DFT in the study of aromaticity. Chemical reviews 101(5), 1451-1464.

Domínguez-Villa, F.X., Durán-Iturbide, N.A., Ávila-Zárraga, J.G., 2021. Synthesis, molecular docking, and in silico ADME/Tox profiling studies of new 1-aryl-5-(3-azidopropyl) indol-4-ones: Potential inhibitors of SARS CoV-2 main protease. Bioorganic chemistry 106, 104497.

Eşme, A., Sağdınç, S.G., 2018. Molecular structures, spectroscopic (FT–IR, NMR, UV) studies, NBO analysis and NLO properties for tautomeric forms of 1, 3-dimethyl-5-(phenylazo)-6-aminouracil by density functional method. Spectrochimica Acta Part A: Molecular and Biomolecular Spectroscopy 188, 443-455.

Finkel, T., 2011. Signal transduction by reactive oxygen species. Journal of Cell Biology 194(1), 7-15.

Guengerich, F.P., 2008. Cytochrome p450 and chemical toxicology. Chemical research in toxicology 21(1), 70-83.

Kittakoop, P., Mahidol, C., Ruchirawat, S., 2014. Alkaloids as important scaffolds in therapeutic drugs for the treatments of cancer, tuberculosis, and smoking cessation. Current topics in medicinal chemistry 14(2), 239-252.

Kombo, D.C., Tallapragada, K., Jain, R., Chewning, J., Mazurov, A.A., Speake, J.D., Hauser, T.A., Toler, S., 2013. 3D molecular descriptors important for clinical success. Journal of chemical information and modeling 53(2), 327-342.

Koopmans, T., 1934. Über die Zuordnung von Wellenfunktionen und Eigenwerten zu den einzelnen Elektronen eines Atoms. physica 1(1-6), 104-113.

Lien, E.J., Guo, Z.-R., Li, R.-L., Su, C.-T., 1982. Use of dipole moment as a parameter in drug–receptor interaction and quantitative structure–activity relationship studies. Journal of pharmaceutical sciences 71(6), 641-655.

Lovering, F., Bikker, J., Humblet, C., 2009. Escape from flatland: increasing saturation as an approach to improving clinical success. Journal of medicinal chemistry 52(21), 6752-6756.

Macalino, S.J.Y., Gosu, V., Hong, S., Choi, S., 2015. Role of computer-aided drug design in modern drug discovery. Archives of pharmacal research 38, 1686-1701.

Małkiewicz, M.A., Szarmach, A., Sabisz, A., Cubała, W.J., Szurowska, E., Winklewski, P.J., 2019. Blood-brain barrier permeability and physical exercise. Journal of neuroinflammation 16, 1-16.

Manikandan, P., Nagini, S., 2018. Cytochrome P450 structure, function and clinical significance: a review. Current drug targets 19(1), 38-54.

Mebi, C.A., 2011. DFT study on structure, electronic properties, and reactivity of cis-isomers of [(NC 5 H 4-S) 2 Fe (CO) 2]. Journal of Chemical Sciences 123, 727-731.

Olofinsan, K., Abrahamse, H., George, B.P., 2023. Therapeutic role of alkaloids and alkaloid derivatives in cancer management. Molecules 28(14), 5578.

Paladhi, A.G., Pandita, A., Manohar, M., Inamdar, B., Vallinayagam, S., Pandita, D., Murthy, K.S., 2023. Camptotheca acuminata Decne, Potent Anticancer Medicinal Plants. Apple Academic Press, pp. 131-150.

Rashid, M., Afzal, O., Altamimi, A.S.A., 2021. Benzimidazole molecule hybrid with oxadiazole ring as antiproliferative agents: In-silico analysis, synthesis and biological evaluation. Journal of the Chilean Chemical Society 66(2), 5164-5182.

Savjani, K.T., Gajjar, A.K., Savjani, J.K., 2012. Drug solubility: importance and enhancement techniques. International Scholarly Research Notices 2012(1), 195727.

Serin, S., 2022. DFT-based computations on some structurally related N-substituted piperazines. Journal of the Indian Chemical Society 99(11), 100766.

Shahab, S., Sheikhi, M., 2020. Antioxidant properties of the phorbol: a DFT approach. Russian Journal of Physical Chemistry B 14, 15-18.

Sharma, A., Narang, A., Kumar, N., Rana, R., Megha, Pooja, Dhir, M., Gulati, H.K., Jyoti, Khanna, A., 2025. CADD based designing and biological evaluation of novel triazole based thiazolidinedione coumarin hybrids as antidiabetic agent. Scientific Reports 15(1), 4302.

Singh, A., Ansari, K., Banerjee, P., Murmu, M., Quraishi, M., Lin, Y., 2021. Corrosion inhibition behavior of piperidinium based ionic liquids on Q235 steel in hydrochloric acid solution: experimental, density functional theory and molecular dynamics study. Colloids and Surfaces A: Physicochemical and Engineering Aspects 623, 126708.

Sneader, W., 1996. Drug prototypes and their exploitation. (No Title).

Tandon, H., Ranjan, P., Chakraborty, T., Suhag, V., 2021. Polarizability: A promising descriptor to study chemical–biological interactions. Molecular Diversity 25, 249-262.

Vlad, I.M., Nuta, D.C., Chirita, C., Caproiu, M.T., Draghici, C., Dumitrascu, F., Bleotu, C., Avram, S., Udrea, A.M., Missir, A.V., 2020. In silico and in vitro experimental studies of new dibenz [b, e] oxepin-11 (6 H) one O-(arylcarbamoyl)-oximes designed as potential antimicrobial agents. Molecules 25(2), 321.

Yadav, R., Imran, M., Dhamija, P., Chaurasia, D.K., Handu, S., 2021. Virtual screening, ADMET prediction and dynamics simulation of potential compounds targeting the main protease of SARS-CoV-2. Journal of Biomolecular Structure and Dynamics 39(17), 6617-6632.

Zhang, H., Xu, H., Ashby Jr, C.R., Assaraf, Y.G., Chen, Z.S., Liu, H.M., 2021. Chemical molecular-based approach to overcome multidrug resistance in cancer by targeting P-glycoprotein (P-gp). Medicinal research reviews 41(1), 525-555.

Zheng, Y.-Z., Deng, G., Liang, Q., Chen, D.-F., Guo, R., Lai, R.-C., 2017. Antioxidant activity of quercetin and its glucosides from propolis: A theoretical study. Scientific reports 7(1), 7543.

Zhou, S.-F., 2008. Drugs behave as substrates, inhibitors and inducers of human cytochrome P450 3A4. Current drug metabolism 9(4), 310-322.